

# A DYNAMIC RULE IN CELLULAR AUTOMATA

**C. E. Somarakis**

*PhD Student*  
School of Electrical &  
Computer Engineering,  
National Technical University  
of Athens, GR  
cslakonas@yahoo.gr

**G. P. Papavassilopoulos**

*Professor*  
School of Electrical &  
Computer Engineering,  
National Technical University  
of Athens, GR  
yorgos@netmode.ntua.gr

**F. E. Udwardia**

*Professor*  
Viterbi School  
of Engineering,  
University of Southern  
California, USA  
fudwadia@usc.edu

**Abstract**—In this paper a new rule in cellular automata is introduced. Through phenomenological studies and basic numerical explorations, its generic dynamical behavior is outlined. Properties such as periodic and complex behavior are reported and studied at an elementary level. Further research on the rule is recommended since under certain variations (many of which are reported) this rule can be a reliable model for simulating procedures among various fields of study.

**Index Terms**—Cellular Automata, Phase Transition, Complex Dynamics

## I. INTRODUCTION AND HISTORICAL NOTES

Cellular automata are among the simplest mathematical representations of complex dynamical systems. They are a class of spatially and temporally discrete, deterministic systems characterized by local interaction and an inherently parallel form of evolution. The history of cellular automata can be traced back to 1948, when *J. L. von Neumann* introduced them to study simple biological systems [Neumann(1948)]. As his work progressed, *Neumann* started to cooperate with *S. M. Ulam*, who introduced him to the concept of cellular spaces [Wolfram(2000)]. These described the physical structure of a cellular automaton, i.e., a grid of cells which can be either “on” or “off”. Shortly after, *A. M. Turing* proposed, in 1952, a model that illustrated reaction-diffusion in the context of morphogenesis [Turing(1952)]. In the 1970s, cellular automata found their way to one of the most popular applications called *simulation games*, of which *J. H. Conway’s, Game of Life* is probably the most famous [Gardner(1970)]. However, the widespread popularisation of these systems was achieved in the 1980s through the work of *S. Wolfram*. Based on empirical experiments using computers, he gave an extensive classification of cellular automata as mathematical models for self-organising statistical systems [Wolfram(2000)]. *Wolfram’s* systematic research is to relate cellular automata to all disciplines of science (e.g., sociology, biology, physics, mathematics, economy, etc).

In this paper, we will introduce a new dynamical rule (we shall call it  $\mathcal{F}$ -rule). This model came as a result of comprehensive research in dynamical structures of networks as these were constructed out of game theory and statistical physics. The  $\mathcal{F}$ -rule is an outgrowth of the *Prisoner’s Dilemma* game as it is stated by *Nowak et al* [Nowak and May(1992)]. In fact, the very first introduction of the  $\mathcal{F}$ -rule was in [Wiederien and Udwardia(2004)]. The present paper can be considered as

a continuation of [Wiederien and Udwardia(2004)] where we consider more general games played among the neighbors. We consider the model as a discrete dynamical system evolving in a discrete state space. Our aim is to explore its properties and outline the emerging dynamics and the degree of complexity. For some values of the parameters of the local interaction drastically different behaviors are observed. Our aim is to characterise the long-term behavior in terms of average values as well as the identification of critical values of the parameters where various patterns (behavior or phase transitions) occur.

### A. Notations and Definitions

Before introducing our model, it is necessary to present four generic characteristics of cellular automata. These primary concepts will assist in getting a picture of the rule’s behavior both locally and globally.

1) *The State Space*: We define an space  $\mathcal{L} : \mathbb{N}^d$ , where  $\mathbb{N}$  is the set of natural numbers, as the discrete state space. This is the lattice of  $d$ -dimensional sites upon which our automata live, and their dynamics unfold. Every individual site can be defined by a  $(1 \times d)$  vector  $\vec{x}$ . In this paper, we mainly consider two-dimensional spaces (see Fig. 1(a)).

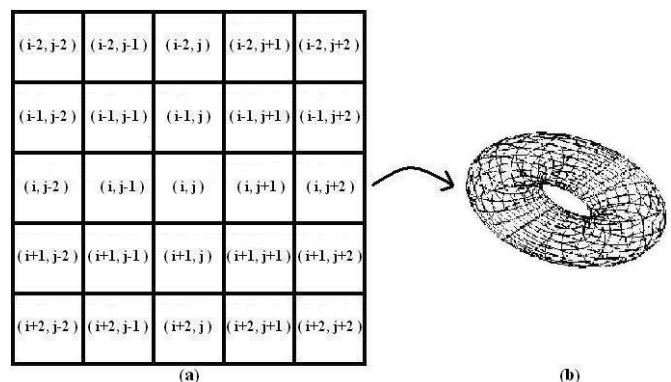


Fig. 1. (a)The plane lattice is the state space of our system. Every cell can be defined as site of a regular 2D matrix. (b)The periodic conditions imply that the opposite edges of the lattice get glued to form a torus.

2) *Local Value Space*: Each cell  $\vec{x} \in \mathcal{L}$  can assume only a finite number of different values:

$$\sigma(\vec{x}; t) \in \Sigma = \{0, 1, 2, \dots, k-1\} \times \mathbb{N} \quad (1)$$

where  $\sigma(\vec{x}; t)$  is the value of  $\vec{x}$  at time  $t \in \mathbb{N}$ . In our paper, we set  $k = 2$ . The set of possible states at time  $t$  can be either  $\sigma = 0$  or  $\sigma = 1$ . In the presented simulations below, a black-coloured site means a site in 0 state, whereas a white-coloured site is in state 1.

3) *Neighbourhood of a cell*: Every cell changes its state after communicating with its neighboring cells. We note by  $\mathcal{N}(\vec{x}, r)$  the range- $r$  neighbourhood of  $\vec{x}$ , without  $\vec{x}$  itself, and by  $\underline{\mathcal{N}}(\vec{x}, r)$  the range- $r$  neighborhood, including  $\vec{x}$ , i.e.

$$\mathcal{N}(\vec{x}, r) = \{\vec{y} \in \mathcal{L} : 0 < \|\vec{x} - \vec{y}\|_\infty < r\} \quad (2)$$

$$\underline{\mathcal{N}}(\vec{x}, r) = \{\vec{y} \in \mathcal{L} : 0 \leq \|\vec{x} - \vec{y}\|_\infty < r\} \quad (3)$$

where  $\|\cdot\|_\infty : \mathbb{N}^d \rightarrow \mathbb{N}$  is the infinity norm. In our work we fix  $r = 1$  which means that for the neighbourhood of a given center site  $\vec{x}$  is the set of sites which are immediately adjacent to  $\vec{x}$ . This scheme is generally known as *Moore scheme* [Wolfram(2000)], [Ilachinski(2002)]. Having defined the basic topology of our lattice, we denote by  $\mathcal{P}(N^2)$  the *power set* of  $\mathcal{L}$ . This is the set of all possible global states  $G(t) = \{\sigma(\vec{x}; t)\} \forall \vec{x} \in \mathcal{L}$  at time  $t$ . For  $k = 2$ ,  $\text{card}\mathcal{P}(N^2) = 2^{N^2}$ .

4) *Boundary Conditions*: Although cellular automata are assumed to live on infinitely large lattices, computer simulations necessarily run on finite sets. Thus, it is also essential to define conditions on the boundaries of the lattices. Among various types of boundary conditions that have been proposed [Wolfram(2000)], [Ilachinski(2002)], in this paper, finite lattices are exclusively considered with *periodic* boundary conditions as depicted in Fig. 1(b).

## B. The $\mathcal{F}$ -Rule

We now move on to define the transition rule under which the states of sites in  $\mathcal{L}$  are updated. To every  $\vec{x} \in \mathcal{L}$ , we assign a cost function  $V(\vec{x}, \mathcal{N}(\vec{x})) : \Sigma^2 \rightarrow W = \{a, b, c, d\} \subset \mathbb{R}$  such that:

$$V(\vec{x}, \vec{y}) = \begin{cases} a & \text{if } \sigma(\vec{x}; t) = \sigma(\vec{y}; t) = 0 \\ b & \text{if } \sigma(\vec{x}; t) = 0, \sigma(\vec{y}; t) = 1 \\ c & \text{if } \sigma(\vec{x}; t) = 1, \sigma(\vec{y}; t) = 0 \\ d & \text{if } \sigma(\vec{x}; t) = \sigma(\vec{y}; t) = 1 \end{cases} \quad (4)$$

The payoff matrix of (4) is as in Fig. 2(a). By this figure, one can perceive a primary physical hypothesis of these cost values. They, in fact, reflect the tension of local interactions between individual cells. So, the initial step of our rule is that for a fixed value  $\sigma(\vec{x}; t)$  and for every  $\sigma(\vec{y}; t)$  of  $\vec{y} \in \mathcal{N}(\vec{x})$  we adjust a number  $w \in W$  to  $\vec{x}$ . For a fixed arrangement of states in  $\mathcal{N}(\vec{x})$ , site  $\vec{x}$  receives an overall cost

$$\mathcal{V} = \sum_{\vec{y} \in \mathcal{N}(\vec{x})} V(\vec{x}, \vec{y}) \quad (5)$$

Finally,  $\forall \vec{x} \in \mathcal{L}, \vec{z} \in \underline{\mathcal{N}}(\vec{x})$  the update rule is defined to be:

$$\sigma(\vec{x}; t+1) = \mathcal{F}(\sigma(\vec{z}; t)) = \sigma(\vec{z}; t)$$

where  $\vec{z}$  is such that

$$\mathcal{V}(\vec{z}) = \max_{\vec{z} \in \underline{\mathcal{N}}(\vec{x})} \mathcal{V}(\vec{z}) \quad (6)$$

In the following, we will symbolize by  $\mathcal{F}_{(a,b,c,d)}$  a sufficiently defined model.

1) *Properties and Remarks*: It can be easily shown that:

$$1. \mathcal{F}_{(a,b,c,d)} \equiv \mathcal{F}_{(a+q,b+q,c+q,d+q)} \quad \forall q \in \mathbb{R} \quad (7a)$$

$$2. \mathcal{F}_{(a,b,c,d)} \equiv \mathcal{F}_{(aq,bq,cq,dq)} \quad \forall q \in \mathbb{R}_+ \quad (7b)$$

These two properties declare the model's invariance under additivity and multiplication, which imply that the dynamics occurring from some range of parameters image a more generic parameter subspace.

At this point, we should make two remarks concerning the nature of this rule. First, this model is a purely deterministic dynamic procedure. Neither stochastic fluctuations, nor any sort of noise, affect the evolution of the cells. Secondly, a careful insight into the rule's local behavior reveals that the interactions are in fact within a range  $r = 2$  rather than  $r = 1$ . In the previous paragraph we noted that the decision of  $\sigma(\vec{x}; t+1)$  depends on the values of  $\mathcal{V}(\vec{z} \in \underline{\mathcal{N}}(\vec{x}))$  at time  $t$ . However, every cost  $\mathcal{V}$  is, subsequently, a result of local interaction between the neighbours of the center site and their own neighbors. What, actually, happens is the local alternation of two, interconnected, procedures. If  $G(t), J(t)$  are the instant global state and cost values of  $\mathcal{L}$  respectively, then  $\mathcal{F}$ -rule can be separated into alternating between sub-rules:

$$\mathcal{F} = \begin{cases} f_1 : G(t) \rightarrow J(t) \\ f_2 : J(t) \rightarrow G(t+1) \end{cases} \quad (8)$$

where  $f_1$  is the function that sets the costs out of the states and  $f_2$  is the function that updates the (new) states out of the costs. Next questions arise intuitively. "What is so interesting about this rule?", "What kind of behavior is this rule capable of exhibiting?". In the following, we will attempt to provide, hopefully intriguing, answers.

## II. EVOLUTION FROM SIMPLE SEEDS

To this extent, we shall furtherly simplify the rule by fixing the cost values  $a = 0, d = 1$  and  $b, c > 0$  that are free to vary. We will provide sufficient evidence that the variation of these two parameters causes intricate phenomena. In this section, we will discuss the spatial evolution of the rule, starting from a specific initial configuration known as *simple seeds*. Here, the lattice consists of a zero-valued (black) site, in a background of non zero-valued (white) sites (see Fig. 2(b1)). The growth of cellular automata from such setup provides models for a variety of physical and other phenomena such as crystal growth [Packard(1985)]. In general, this type of initial conditions will help us to understand the complexity of the rule's dynamics in both space and time.

### A. An analytical approach

Like the vast majority of cellular automata,  $\mathcal{F}$ -rule generates a -simple to understand, difficult to solve- evolution. One will realise this, by simply speculating the rule's formalistic definition (eq. (4)-(6)): three equations for the update of a single cell (!). By the last simplification of the  $\mathcal{F}$ -Rule we have

cut its control parameters down to two ( $b$  and  $c$ ). Nevertheless, it is may be unwise to begin setting arbitrary values for the  $b$  and  $c$  costs. It is highly possible either to keep selecting values that are “not-interesting” or, at least, exhaustingly difficult to organize the potential “interesting” behaviors. The simple seed setup is a, convenient enough, pattern as to run the first steps of the rule “by hand”. In Fig 2(b1) a window of our initial lattice is presented, where every value is at  $\sigma(\vec{y}; 0) = 1$ , apart from the central site  $\vec{x}$  where  $\sigma(\vec{x}; 0) = 0$ . By  $f_1$ , the next step is to assign each site a cost value. In Fig. 2(b1) we present the results for our neighborhood of cells: It is easy to see that due to the symmetry of the pattern the arising costs are:

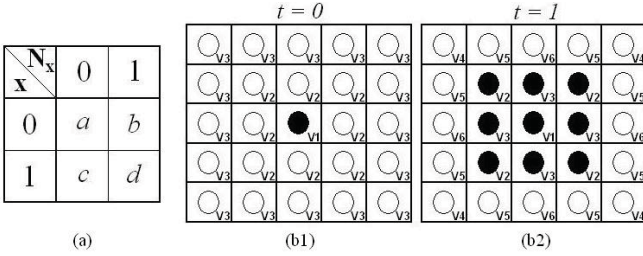


Fig. 2. (a)The  $\mathcal{F}$  payoff table. It is derived from (4) and specifies the effect between contiguous cells. Namely it defines the local interaction of sites at every time step. (b)The simple seed configuration. (c) For  $(b, c)$  values:  $7 + c < 8b$  and  $b > 1$ , zero state expands to its neighbors. Because of the special initial conditions, symmetry is, throughout the evolution, preserved.

$$\left\{ \mathcal{V}_1 = 8b \quad \mathcal{V}_2 = 7 + c \quad \mathcal{V}_3 = 8 \right\}$$

For the remaining cells of the lattice the cost values are, obviously,  $\mathcal{V} = \mathcal{V}_3 = 8$ . Hence, at  $t = 0$  the turn-up costs are  $8b, 7 + c, 8$ . Now, if  $7 + c \geq 8b$  we should expect that our sole site will step to *white* and stay unchanged for the rest of the time. Else, if  $7 + c < 8b \leq 8$  there should be no change in the states of the cells:  $\vec{x}$  has the largest cost among its neighbors  $\mathcal{N}(\vec{x})$ , while the latter cells adjoin to cells with larger than  $\mathcal{V}(x) = \mathcal{V}_1$  costs. Therefore, our pattern remains static forever. The last case is when  $7 + c < 8b$  and  $b > 1$  where we expect that the neighborhood will turn to the one in Fig 2(b2). The costs at  $t = 1$  are:

$$\left\{ \begin{array}{lll} \mathcal{V}_1 = 0 & \mathcal{V}_2 = 5b & \mathcal{V}_3 = 3b \\ \mathcal{V}_4 = 7 + c & \mathcal{V}_5 = 6 + 2c & \mathcal{V}_6 = 5 + 3c \end{array} \right\}$$

The future evolution of our automaton depends on the relative values of the  $b$  and  $c$  parameters as they were set by the  $\mathcal{V}$ -costs. The equalities define the  $(b, c)$  phase transition diagram of the model’s dynamic behavior. In Fig 3(a), we have sketched a raw phase transition pattern on the  $(b, c)$  plane. For the simple-seed setup, seven different schemes have been identified (see Figs. 4 and 5):

- **P1:** The system *directly* (i.e. without transient states) evolves to homogeneous state where all cells attain the same value (i.e.  $\sigma = 1$ ).
- **P2:** The system directly evolves to periodic behavior of period 2.

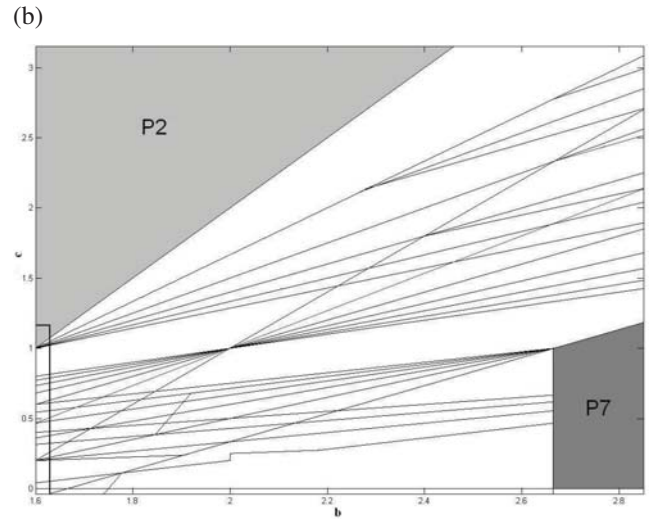
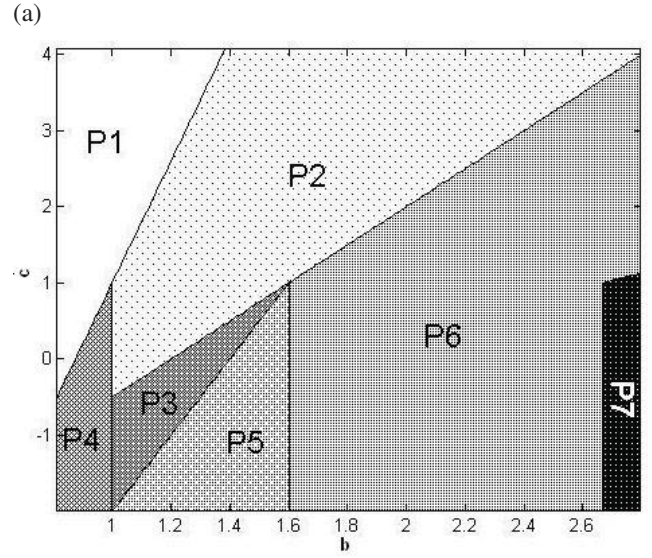


Fig. 3. (a) A characteristic window of the  $(b, c)$ -plane, where we have sketched a generic phase transition diagram. While regions P1,P2,P3,P4,P5 and P7 appear regular dynamics, P6 is rich in irregular behavior (see Fig(1a)).(b) The phase transition diagram of a part of P6 region ( $1.6 < b < 2.85$ ). See text for details. The linear boundaries were numerically estimated. The calculation’s precision is  $10^{-3}$ . The bounded rectangular area shown at the lower left corner of the diagram is thoroughly explored (see §IIB1).

- **P3:** The system directly evolves to periodic behavior of period 3.
- **P4:** The system directly evolves to periodic behavior of period 1.
- **P5:** The system expands in the first iteration and remains static ever after.
- **P6:** The system expands to an irregular complex behavior.
- **P7:** The system expands uniformly. At each time step, a regular pattern with a fixed density of zero sites is produced.

The boundaries of the diagram are, obviously, the set of critical (bifurcation) values. For instance, at the P5, P6 boundary we

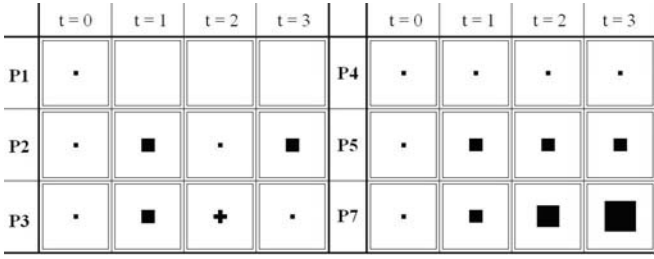


Fig. 4. Dynamic evolution of the *regular* regions of  $(b, c)$ -plane P1,P2,P3,P4,P5,P7. Plain periodic patterns with uniform structure may only appear.

step on the critical vertical line of  $b = 8/5$ . Similarly, the P6 to P7 boundary consists of the connected lines  $b = 8/3$  and  $c = b - 5/3$ . These values together with the rest of the limit lines have been, analytically, derived from the above procedure. We directly realize, though, that it only takes few steps for the system to become forbiddingly complicated towards any analytic approach. So we have no choice but running computer simulations for any further analysis. For the moment we are, primarily, interested in investigating this “irregular” P6 region.

### B. The P6 region

Contrary to the other sections, P6 is a parameter subspace, where the automaton appears to exhibit extraordinary dynamics. Characteristic images of this region are presented in Fig. 5. Unlike the other six regions, patterns have no simple faceted form and in most cases non-uniform interior. Additionally, due to symmetric initial states, these patterns are completely invariant under all the rotation and reflection symmetry transformations. In order to identify part of the P6 dynamics, we implemented various techniques presented below. Our first step was to numerically estimate the P6 transition phase space, a part of which is presented in Fig. 3(b). At first sight, one may observe that P6 is a collection of mutually disjoint subsets of  $(b, c)$ -plane. These subsets have occurred out of subsequent straight line intersections. This is an expected outcome, if one intuitively expands those first steps of the algorithm back in §IA. In each of these subsets, our system generates the same pattern and, of course, exhibits the same dynamic behavior. So the following question would be “What is this dynamic behavior?”.

1) *Global dynamics on a finite, fixed  $\mathcal{L}$* : Our first approach was to keep the lattice size constant at  $N=50$ . On this  $50 \times 50$  space  $\mathcal{L}$  with periodic boundaries, we explored the system’s long term behavior selecting cost values from the rectangular sketched in Fig. 3(b). Each simulation test was run for at most 20,000 iterations. The observed results are classified in three qualitative classes:

- A After a transient behavior, all sites of  $\mathcal{L}$ , eventually, attain the same value.
- B After a transient behavior, all sites of  $\mathcal{L}$ , converge to *periodic (period- $T$ )* motion. There

$\exists t_{trans} \in \mathbb{N} : \sigma(G; t) = \sigma(G; t + T) \forall t < t_{trans}$  where  $G \in \mathcal{P}(N^2)$ .

- C The dynamic evolution does not converge to any of the previous two classes. A typical C-class behavior is the one that after a sufficiently large number of iterations (20,000) the pattern neither, strictly, repeats itself, nor turns out to a homogeneous state.

In Table I, we present the numerical results in details.

Class	Parameter $c$ range	Transient time ( $t_{trans}$ )	Steady state ( $t > t_{trans}$ )
A	(0.0000, 0.0059)	100	$\sigma(G; t) = 0$
A	(0.0600, 0.2062)	643	$\sigma(G; t) = 0$
A	(0.2063, 0.2166)	1388	$\sigma(G; t) = 0$
C	(0.2167, 0.2374)	-	<i>no convergence</i>
C	(0.2375, 0.2999)	-	<i>no convergence</i>
B	(0.3000, 0.3285)	872	$\sigma(G; t) = \sigma(G; t + 2)$
B	(0.3286, 0.3899)	118	$\sigma(G; t) = \sigma(G; t + 2)$
C	(0.3900, 0.4124)	-	<i>no convergence</i>
C	(0.4125, 0.4916)	-	<i>no convergence</i>
B	(0.4917, 0.5333)	2569	$\sigma(G; t) = \sigma(G; t + 4)$
B	(0.5334, 0.5642)	802	$\sigma(G; t) = \sigma(G; t + 4)$
B	(0.5643, 0.6187)	1111	$\sigma(G; t) = \sigma(G; t + 12)$
B	(0.6188, 0.6499)	2935	$\sigma(G; t) = \sigma(G; t + 4)$
B	(0.6500, 0.7199)	914	$\sigma(G; t) = \sigma(G; t + 6)$
B	(0.7200, 0.7666)	515	$\sigma(G; t) = \sigma(G; t + 6)$
B	(0.7667, 0.7999)	299	$\sigma(G; t) = \sigma(G; t + 6)$
B	(0.8000, 0.8249)	199	$\sigma(G; t) = \sigma(G; t + 4)$
B	(0.8250, 1.0357)	494	$\sigma(G; t) = \sigma(G; t + 4)$
B	(1.0358, 1.0416)	40	$\sigma(G; t) = \sigma(G; t + 2)$
B	(1.0417, 1.0490)	77	$\sigma(G; t) = \sigma(G; t + 2)$
B	(1.0500, 1.0624)	33	$\sigma(G; t) = \sigma(G; t + 2)$
B	(1.0625, 1.0833)	22	$\sigma(G; t) = \sigma(G; t + 2)$
B	(1.0834, 1.1249)	29	$\sigma(G; t) = \sigma(G; t + 2)$

TABLE I  
\*

Results from numerical exploration of the bounded phase transition area in Fig. 3(b). For each subset of the diagram we generated simple seed pattern and let the simulation run for approx. 20,000 iterations. The results are presented above. In most cases our system falls in periodic states after some transition time, while other control values of  $(b, c)$  generate patterns that seem not to converge. Note that the maximum number of iterations is much greater than the maximum transient time reported. This secures somehow the reliability of our analysis. One should not expect an everlasting aperiodic evolution on a finite space  $\mathcal{L}$ , anyway.

### C. Complex Behavior

In this section, we will provide sufficient evidence to argue that our automaton is rightfully characterized as complex. The cost parameters come mainly from the P6 region, although another cost setup is also presented. The system initiates from a simple-seed configuration and evolves on a large size (practically infinite) matrix  $\mathcal{L}$ .

1) *Stability*: An important qualitative characterization of complex behavior in deterministic dynamical systems is their sensitivity to small changes made to the initial states. A convenient measure for quantifying the divergence between evolutions starting from two similar binary valued global states,  $\sigma(G_1)$  and  $\sigma(G_2)$  is the *Hamming distance*,

$$H_{\sigma(G_1), \sigma(G_2)}(t) = \sum_{i,j=1}^N \sigma((i, j)_1; t) \oplus_2 \sigma((i, j)_2; t) \quad (9)$$

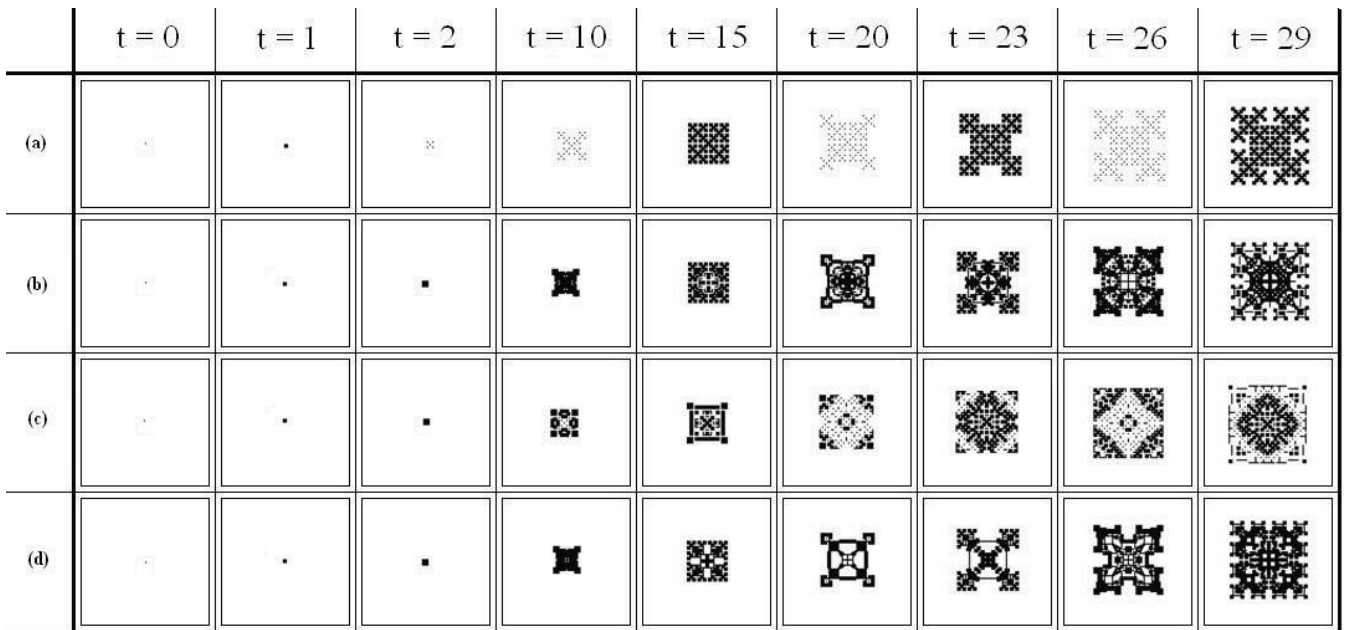


Fig. 5. Examples of classes of patterns generated by evolution of  $\mathcal{F}$ -rule. For each of these automata, a sequence of frames shows the two-dimensional configuration and evolution. (a)  $\mathcal{F}_{(0,1.65,1.0834,1)}$ , (b)  $\mathcal{F}_{(0,1.65,0.4125,1)}$ , (c)  $\mathcal{F}_{(0,2.6,0.2252,1)}$ , (d)  $\mathcal{F}_{(0,1.7,0.4,1)}$

where  $\oplus_2$  is the *modulo-2* sum operator.

Hamming distance is a fundamental measure in Coding Theory and has already been used in 1-D cellular automata to primarily characterise the emerging difference from two *nearby* initial configurations [Wolfram(2000)]. These configurations are patterns that differ at only one site value (i.e.  $H(0) = 1$ ). Suppose that  $G_1$  and  $G_2$  are global configurations which differ at one site. For simple update rules, the difference remains localized to a few sites, and the total Hamming distance tends rapidly to a small constant value or remains bounded. On the other hand, complex rules generate a growing with time  $H(t)$  curve. This implies their instability to small perturbations. This is the case presented in Fig. 6. There,  $\mathcal{F}_{(0,1.65,1.0834,1)}$  unfolds on a  $560 \times 560$  square space. The 6(b) plot depicts this *rapid* divergence of nearby initial setups. The average Hamming distance, smoothed over many time steps, behaves as  $H(t) \propto t^{1.95}$ . As it is stated in [Wolfram(2000)], [Ilachinski(2002)], in case of one-dimensional cellular automata, unbounded  $H(t)$  characterizes rules that generate chaotic patterns.

2) *Growth Dimensions*: The limiting structure of patterns generated by the growth of cellular automata from simple seeds can be characterized by various *growth dimensions*. Growth dimensions, in general, describe the logarithmic asymptotic scaling of the total sizes of patterns with their linear dimensions. The type of dimension we will make use of depends on the *boundary* of the pattern. The boundary may be defined as the set of black sites that can be reached by some path on the lattice that begins at “infinity” and does not cross any zero (black) sites. This set of limiting cells can thus be

found by a simple recursive procedure:

$$D_g = \lim_{t \rightarrow \infty} \frac{\log \bar{N}(t)}{\log t} \quad (10)$$

Where  $\bar{N}(t)$  is the number of boundary (black) cells of our system at time  $t$ . In Fig. 6a we see the evolution of  $\mathcal{F}_{(0,1.65,1.0834,1)}$  and the dendritic geometry of its boundaries. In Fig. 6c we present this logarithmic plot in which  $D_g = 1.8 \pm 0.1$ .

3) *Space-Time Patterns*: A direct and most applicable technique of examining an asymptotical behavior is through a state subspace analysis. One may choose to define *Poincaré*-like sections and study the dynamic evolution of this subspace. Specifically, we consider the center horizontal or the diagonal line of the two-dimensional lattice with time (see Fig. 9(a)). The reason we choose these specific sections is rather intuitive. They are the two axes of symmetry and a view of their evolution in time would be most enlightening. In Figs. 7(b) and 7(c) we present examples of space-time patterns from the center-horizontal and diagonal lines, respectively. Fig. 7(b) presents the dynamics of rule  $\mathcal{F}_{(0,1.61,0,1)}$  after 250 iterations. The evolution converges to this scale invariant, image. Its fractal dimension is estimated at  $D_F = 1.882 \pm 0.002$ . In Fig. 7(c) we present the pattern generated by  $\mathcal{F}_{(0.5,0.4,1,0.22)}$ . This rule produces the well-known *Sierpiński gasket*, the dimension of which is analytically calculated at  $D_F = \ln(3)/\ln(2) \approx 1.585$ . It is worth mentioning that the diagonal space-time pattern of that rule is identical to the elementary (1D) cellular automata (**R154**), considering Wolfram’s notation [Wolfram(2000)].

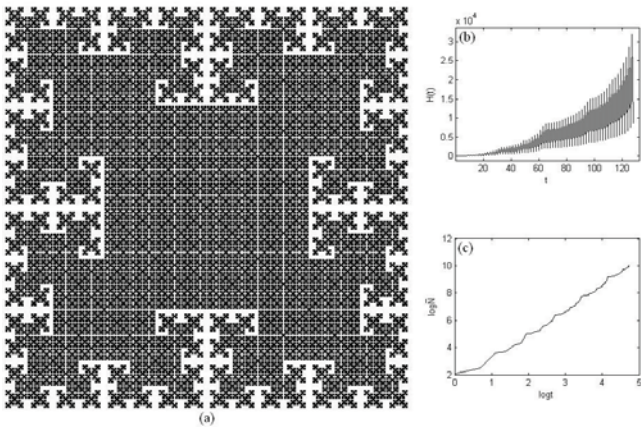


Fig. 6. Rule  $\mathcal{F}_{(0,1.65,1.0834,1)}$ . (a) Evolution on a  $560 \times 560$  lattice. Although the interior appears uniform structure, it's boundary shapes dendritic curve.(b) The Hamming distance of the rule as it results from two, almost similar, initial configurations. Here  $H(t) \propto t^{1.95}$  which indicates high sensitivity to initial conditions.(c) The logarithmic plot of eq. (10) reveals the model's scaling law between boundary cells and time. The slope gives an estimation of the growth dimension  $D_g \approx 1.8$ .

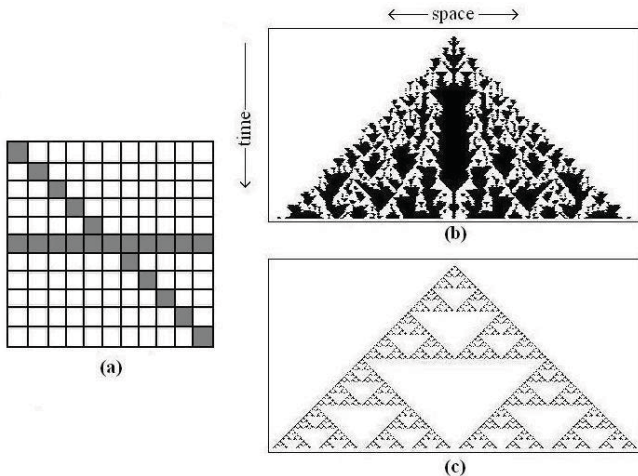


Fig. 7. (See text for details.) (a) The space time pattern method to identify complex in 2D cellular automata. As the system process its dynamics on the lattice a useful technique is to isolate a line of cells and watch their progress separately [Wolfram(2000)]. A reasonable choice is this of the center horizontal or the diagonal line.(b) A space-time section of  $\mathcal{F}_{(0,1.61,0,1)}$  shows the evolution of the center horizontal line of sites. The generated pattern asymptotically converges to a self-similar object.(c) Diagonal space-time pattern of  $\mathcal{F}_{(0.5,0.4,1,0.22)}$ . The system results in a familiar fractal.

### III. EVOLUTION FROM RANDOM SEEDS

A random seed configuration results when each site  $\vec{x} \in \mathcal{L}$  chooses to be black or white with probability  $p = 1/2$ . This is what is referred as *completely disordered* global state. Such disordered configurations are typical members of the set of all possible configurations. Patterns generated from them are thus typical of those obtained with any initial state. The presence of structure in these patterns is an indication of self-organization on the lattice [Wolfram(2000)]. This type of evolution, though very important, is beyond the scopes of this work. However,

for consistency reasons, we will report a few preliminary results coming out of some superficial explorations. Qualitatively speaking, three types of collective behaviors have been identified. The first one is this when the system sharply converges to a static equilibrium (Fig. (8a)). The second is when, after a transient state, the system converges to a periodic attractor, where the period appears to (perhaps sensitively) depend on the initial conditions (Fig. (8b)). The third is when the system, after thousands of iterations, still exhibits aperiodic behavior (Fig. (8c)). This classification is pretty resemblant to that in §IIB1. A visual inspection of Figs. 8a-c is enough for someone to observe the striking similarities of these patterns to those generated from the probabilistic *Ising* spin model [Ising(1925)], [Kindermann and Snell(1980)]. In any case, further research is, required, especially from a global point of view.

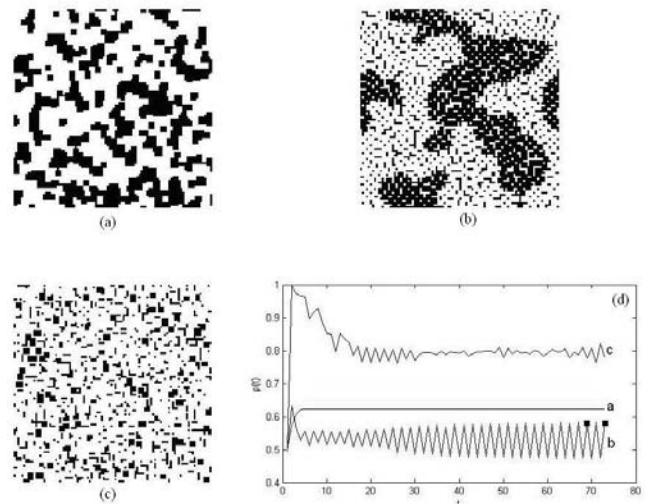


Fig. 8. Patterns generated from random initial conditions. (a)  $\mathcal{F}_{(1,0,0,1)}$ : The system rapidly reaches an equilibrium state of black and white neighborhoods (see subfig. (d) index  $\rho(t)$  curve (a)). (b)  $\mathcal{F}_{(0,1,1,0)}$ : The system generates large amplitude oscillatory behaviors. After a transient mode the system converges to periodic attractors (here period-4, see black dots in subfig.(d)). (c)  $\mathcal{F}_{(0.5,0.4,1,0.22)}$ : The system behaves aperiodically. Weak oscillatory behavior leads to aperiodic evolution.(d) Index  $\rho(t)$ . It is defined as the instant ratio of white cells to the total number of sites.

### IV. DISCUSSION AND CONCLUDING REMARKS

Up to this point, an extensive effort to explore a proposed mathematical model is made. In this section, we will make suggestions for further research on this model. Furthermore, we shall propose types of variations which we believe are of special interest. In the end, we will outline fields on which such model may be applicable.

#### A. Where do we go from here?

In this preliminary paper, our purpose was to study a new update rule in cellular automata and to shed light upon its perspectives. However, many more things are left to do. One line of research could be on the direction of phase transition diagrams which we outlined above. Another issue is this

of dynamic complexity. The Hamming measure used in this paper provides a necessary but not sufficient condition of chaos. Nearby trajectories may diverge in time but this does not mean that either this divergence is exponential, or that it is independent of initial configurations. A more elaborate mathematical tool would be the discrete *Green function*. In cellular automata theory, this function is applied to *difference plots*, out of which quantities analogous to *Lyapunov exponents* are, at least heuristically, derived [Wolfram(2000)], [Ilachinski(2002)]. A different perspective that was, briefly, presented above, is the evolution from a random setup. This point of view requires, in principle, an analysis on the base of global state transitions. We must enhance our armory with mathematical equipment from *Statistical Physics* and *Markov Random Fields* [Wolfram(2000)], [Kindermann and Snell(1980)].

### B. Variations of the $\mathcal{F}$ -rule

Perhaps, the most significant advantage of this model, is its structural flexibility. Conventional variations of cellular automata are the various definitions of neighborhoods  $\mathcal{N}(\vec{x}, r)$  (*Moore* or *Von Neumann* scheme, among others [Ilachinski(2002)]) or the state space topology (e.g. boundary conditions), the dimensionality of the rule ( $\mathcal{L}^d$ ) or perhaps the number of elements in  $\Sigma$ . Apart from typical changes we can also vary our rule in terms of:

*Cost function  $f_1$ .* In this paper we assumed that at the end of every iteration, costs are reset to zero. Namely, we made use of instant costs upon the update decision of cells. A variation with physical meaning would be this of accumulative or discount costs per iteration. Each cell saves its cost values from previous states adding it on the future payoffs. For every iteration, a constant discount factor is multiplied with all past costs before the new cost is added. Preliminary simulations have revealed that the collective behavior of such automata is totally different.

*Decision function  $f_2$ .* We have assumed that the update rule defines the new state of site  $\vec{x} : \sigma(\vec{x}; t+1)$  to equal to the state of its neighbor with the maximum cost. An important variation of  $f_2$  would be this in which every  $\vec{x} \in \mathcal{L}$  to do the following: It calculates the average cost among its bad neighbors and the average cost among its good neighbors. Then  $\vec{x}$  decides to step to the state with the highest average cost. Of course, function  $f_2$  could be configured to decide according to the minimum of costs. Such behaviors may also be observed in practice.

### C. Applications

This automaton could reliably simulate procedures in many fields of life, some of which are reported below:

#### Social networks

If we consider  $\mathcal{L}$  to be a compact society of people (cells), then white,  $\sigma = 1$ , state would adjust to a *good* man while the black,  $\sigma = 0$ , would adjust to the *bad* man. Our lattice is, thus, a collection of concrete neighborhoods which interact, according to a cost function (eq. (4) or Fig. 2(a)), locally and

eventually globally. So let's consider the neighborhood  $\mathcal{N}(\vec{x})$  of cells. Suppose that  $\vec{x}$  is a good man with  $s$  also good neighbors and  $(8 - s)$  bad neighbors. Then, for every good  $\vec{y} \in \mathcal{N}(\vec{x})$ ,  $\vec{x}$  gains a reward of  $d$  units while for every bad, our hero may get a penalty of  $c$  units. From this point of view, table cost is a locomotive regulator of interactions of "good" over "bad" and vice versa. Together with this regulator one can define static controllers as fixed regions of sites (perhaps on the boundary) whose value remain unchanged throughout simulation. Such areas would imitate the role of a church or a police station around a neighborhood.

#### Economic Networks

Modelling market interaction. Economics is a subject of social networks, in which the procedure of learning or imitation and then reply among interacting individuals is fundamental (a game theory approach can be found here [Cartwright(2007)]). In  $\mathcal{F}$ -realm, sites would be sellers and buyers. To make this more intriguing one could raise the number of possible states and then separates them in two categories: people who sell certain goods, and of people who buy them. Cost values would form the relative value between goods.

#### Other applications

We shall briefly report potential applications in physical (statistical mechanics - lattice gas theory) [Kindermann and Snell(1980)], [U. Dieckmann and Metz(2000)] or biological (interaction between malignant and non-malignant cells) networks as well as in computer networks. However in each field further research on this model is required.

### D. Conclusions

In this paper, we studied a model in cellular automata and presented our results. We attempted to shed light upon its dynamics by presenting some of its basic characteristics. Despite the fact that our research focused on a simplified version initiating from a specific type of initial configuration, our model revealed a great degree of spatial and time complex behavior. Finally, we proposed nontrivial variations of the rule that could have significant impact on the evolutionary dynamics and discussed possible applications.

### REFERENCES

- [Cartwright(2007)] Cartwright, E., 2007, Int. J. Game Theory **36**, 116.
- [Gardner(1970)] Gardner, M., 1970, Scientific American , 120.
- [Ilachinski(2002)] Ilachinski, A., 2002, *Cellular Automata. A Discreet Universe* (World Scientific, NJ).
- [Ising(1925)] Ising, E., 1925, Z. Physik **31**, 235.
- [Kindermann and Snell(1980)] Kindermann, J., and J. Snell, 1980, *Markov Random Fields and Their Applications* (AMS, NY).
- [Neumann(1948)] Neumann, J. V., 1948, *Cerebral Mechanisms in Behavior - The Hixon Symposium* , 1.
- [Nowak and May(1992)] Nowak, A., and R. May, 1992, Nature **359**, 826.
- [Packard(1985)] Packard, N., 1985, Institute for Advanced Study (preprint).
- [Turing(1952)] Turing, A., 1952, Phil. Trans. R. Soc. London **237**(641), 37.
- [U. Dieckmann and Metz(2000)] U. Dieckmann, R. L., and J. Metz, 2000, *The Geometry of Ecological Interactions: Simplifying Spatial Complexity* (Cambridge University Press, UK).
- [Wiederien and Udwardia(2004)] Wiederien, R., and F. Udwardia, 2004, Int. J. Bifurcation and Chaos **14**(8), 2555.
- [Wolfram(2000)] Wolfram, S., 2000, *Automata and Complexity. Collected Papers* (Addison-Wesley).